III-nitride blue and UV photonic crystal light-emitting diodes

J. Shakya[a], K. H. Kim[a], T. N. Oder[b], J.Y. Lin[a] and H.X. Jiang*[a]
[a]Department of Physics, Kansas State University, Manhattan, Kansas 66506-2601, USA;
[b]Department of Physics and Astronomy, Youngstown State University, Youngstown, Ohio 44555, USA

ABSTRACT

We report on the successful nano-fabrication and characterization of III-nitride blue and ultraviolet (UV) photonic crystal light emitting diodes (PC-LEDs) using electron beam lithography and inductively coupled plasma dry etching. Triangular arrays of holes with different diameters/periodicities were etched on the LEDs. Optical measurements on the photonic crystals (PCs) performed using near-field scanning optical microscopy (NSOM) showed a 60^o periodic variation with the angle between the propagation direction of emission light and the PCs lattice. Under optical pumping, an unprecedented enhancement factor of 20 in emission light intensity of wavelength 475 nm was achieved at room temperature with emission light parallel to the Γ-K direction of the PCs lattice. Guided by the optical pumping results, new design geometry of LEDs with PCs has been employed to optimize the light extraction. Enhancement in optical power of current injected blue and UV PC-LEDs over conventional LEDs is discussed. It was observed that the optical enhancement factor depends strongly on the PC lattice constant and hole size. The achievement of nitride photonic crystal emitters with enhanced light extraction efficiency is expected to benefit many new applications of III-nitrides including solid-state lighting for general illumination and photonic integrated circuits operating in the visible and UV spectral regions.

Keywords: Photonic Crystals, III-nitride wide bandgap semiconductors, Light-emitting diodes, UV LEDs, blue LEDs, NSOM , PC-LEDs.

1. INTRODUCTION

The recent progresses in high-brightness light-emitting diodes (LEDs) based on III-nitride wide bandgap semiconductors place LED as a strong candidate for solid-state lighting technology. Due to their low power consumption[1], smaller size, and long lifetime as compared to conventional lamps, these LEDs could advantageously replace conventional incandescent as well as florescent lamps for general lighting. In addition, visible LEDs with high external efficiency are currently in high demand for a variety of applications including flat panel displays, printers, and optical interconnects in computers. High efficiency ultraviolet (UV) emitters are particularly sought for applications including chemical and biological agent detection and medical uses. High intensity and high speed UV-LEDs could also be used as transceivers for covert non-line-of-sight (NLOS) optical communications. However, while the internal quantum efficiency (QE) of visible LEDs is close to 100%; most of the light is lost due to the parasitic absorption of lateral guided modes in the semiconductor materials and only about $1/(4n^2)$ of the light emitted radiates through the top and the bottom[2]. For nitride materials, only about 5% of the blue/green light (refractive index $n \sim 2.4$) and about 4% of the UV light (refractive index $n \sim 2.6$) generated in the active region is extracted from the top and the bottom surfaces. The need for improvement of extraction efficiency in LEDs is exceptionally great, especially for deep UV LEDs ($\lambda <$ 300 nm) based on III-nitride wide bandgap semiconductors, which presently have very low QE. Much effort has been exerted in improving LED QE including the use of photon recycling schemes[3] and novel geometrical designs aimed at enlarging escape cones of emitted light[4,5], modifying spontaneous emission by resonant cavity[6], or two dimensional (2D) photonic crystals (PCs)[7,8,9,10,11,12,13,14]. Our group has also previously developed interconnected microdisk LED architecture as a method of enhancing extraction efficiency[15].

Photonic crystals (PCs) have recently attracted much interest since the pioneering work of Yablonovitch[16]. Periodic arrays of holes are typically etched in semiconductors to realize two dimensional (2D) PCs that forbid certain

Fourth International Conference on Solid State Lighting, edited by Ian T. Ferguson, Nadarajah Narendran, Steven P. DenBaars, John C. Carrano, Proc. of SPIE Vol. 5530 (SPIE, Bellingham, WA, 2004) · 0277-786X/04/$15 · doi: 10.1117/12.565632

electromagnetic radiation in the lateral direction creating so called "photonic band gaps" (PBGs) in the plane. This can be exploited to confine light propagation to only the vertical direction and thus enhance light extraction efficiency in LEDs. Ideal PBG is achieved by periodicity in 3 dimensions but for extraction of light in LEDs, it is sufficient to eliminate light propagation in the horizontal plane with the use of 2D PCs. The PBG is determined by lattice periodicity *a* and the diameter *d* of the air holes. Very little work in PCs involving the III-nitride materials in the blue/green and UV wavelengths has been reported due in part to the difficulty in fabrication associated with the required nanometer scale periodicity.

We have obtained a 20-fold enhancement of light extraction by PCs using optical pumping at room temperature in the nitride materials at 475 nm[11]. Optical measurements were performed using near-field scanning optical microscopy (NSOM) uniquely configured for UV wavelengths. A 60^o periodic variation of the optical intensity with the angle between the propagation direction of emission light from the MQW and the PC lattice was observed. Recently, we also reported optical power enhancement of 300 x 300 μm^2 unpackaged LED chips under 20 mA current injection by 63% and 95% in blue (460 nm) and UV (340 nm) PC-LEDs, respectively[12]. Initially, 2D PCs were formed everywhere (including the metal transparent layer) except the contact pads on 300 x 300 μm^2 square shaped LEDs, which does not consider the difference in the symmetry of LEDs with that of PCs and has no distinction between light generation region and extraction region. Here, we report a new design geometry of LEDs and PCs as well as the lattice constant and hole size dependence of the optical power enhancement factor in III-nitride UV LEDs. The new design is guided by the optical pumping configuration that provides a maximum 20-fold enhancement of light extraction by PCs. In the optimized optical pumping configuration, the light generation region (pump spot) was separated from the light extraction region (PCs) and the extraction efficiency was strongly dependent on the angle between the propagation direction of emission light and the PCs lattice[11]. The incorporation of 2D PCs on III-nitride LEDs has been shown to not only significantly enhance the light output of the LEDs[11, 12, 14], but also improve the modulation speed of the LEDs. Our results from picosecond time-resolved EL spectroscopy on UV PC-LEDs reveal a significant increase in the modulation speed of LEDs with PC formation[17]. The increase in the modulation speed of LEDs is primarily due to enhanced surface recombination. Moreover, we have also observed a slight narrowing of the far field emission pattern in PC-LEDs[17].

2. EXPERIMENT

2.1 Growth and fabrication

All the III-nitride structures used were grown by metalorganic chemical vapor deposition (MOCVD) on sapphire substrates. The sources used were trimethylgallium for Ga, trimethylaluminum for Al, trimethylindium for In and ammonia for nitrogen. For Mg doping, bis-cyclopentadienyl-magnesium was transported into the growth chamber during growth while SiH_4 was used for Si doping. For blue LEDs, the InGaN/GaN MQWs were grown by MOCVD on a double side polished sapphire substrate. A 30 nm low temperature AlN buffer layer was first deposited, followed by a 3 μm thick GaN layer. Five periods of $In_{0.2}Ga_{0.8}N$(3nm)/GaN(20nm) MQWs were then grown between a pair of 20 nm thick GaN cladding layers. The PCs were fabricated using electron beam lithography and ICP dry etching. Triangular lattice patterns of circular holes with different diameters *d* from 60 to 140 nm and different periodicity *a* from 120 to 300 nm were defined in an area of about 12 μm x 12 μm on poly-methylmethacrylate (PMMA) initially spun on the nitride samples. The samples were then developed in a solution of methyl isobutyl ketone (MIBK) and isopropyl alcohol (IPA). Subsequent dry etching was performed for 30 seconds using ICP.

Fig. 1(a) shows the schematic diagrams of our 460 nm blue LEDs structure. The active region for the blue LEDs was an $In_{0.2}Ga_{0.8}N$/GaN single quantum well (SQW). Out of these materials, conventional broad area LEDs of 300 x 300 μm^2 were fabricated by standard photolithography and inductively coupled plasma (ICP) dry etching. Fig. 1(b) shows the schematic diagrams of our 333 nm UV LED structure with LED mesa and contact pads. The active region for the UV LEDs was an $Al_{0.11}In_{0.03}Ga_{0.86}N/Al_{0.2}In_{0.03}Ga_{0.77}N$ double quantum well (DQW). Beside the 333 nm UV LEDs, PCs were also incorporated on UV LEDs with slightly different structures and wavelengths λ = 313 nm and λ = 299 nm. Hexagonal mesa of side length 120 μm, as shown in Fig 1(c), was defined by electron beam (e-beam) lithography and etched by ICP dry etching. A hexagonal p-contact pad with 60 μm side length was deposited at the center of the LED mesa. To improve the electrical transport, a 10 μm wide n-type ohmic contact was deposited around

the mesa along with a 100 x 100 μm^2 n-contact pad. Further details of the fabrication procedures are described elsewhere[18].

PCs with triangular lattice patterns of circular holes with varying diameter d = 100 nm to d = 450 nm and periodicity *a* = 300 nm to *a* = 700 nm were fabricated on the LED everywhere (including the metal transparent layer) except the contact pads using e-beam lithography and ICP dry etching as described above. Extraction of guided light traveling along Γ-K direction can be as much as 3 times more than the light traveling along Γ-M direction of the PCs in the nitride quantum well[11]. For efficient extraction of the guided light, Γ-K direction of the PCs was set perpendicular to the sides of the hexagonal mesa in case of UV LEDs.

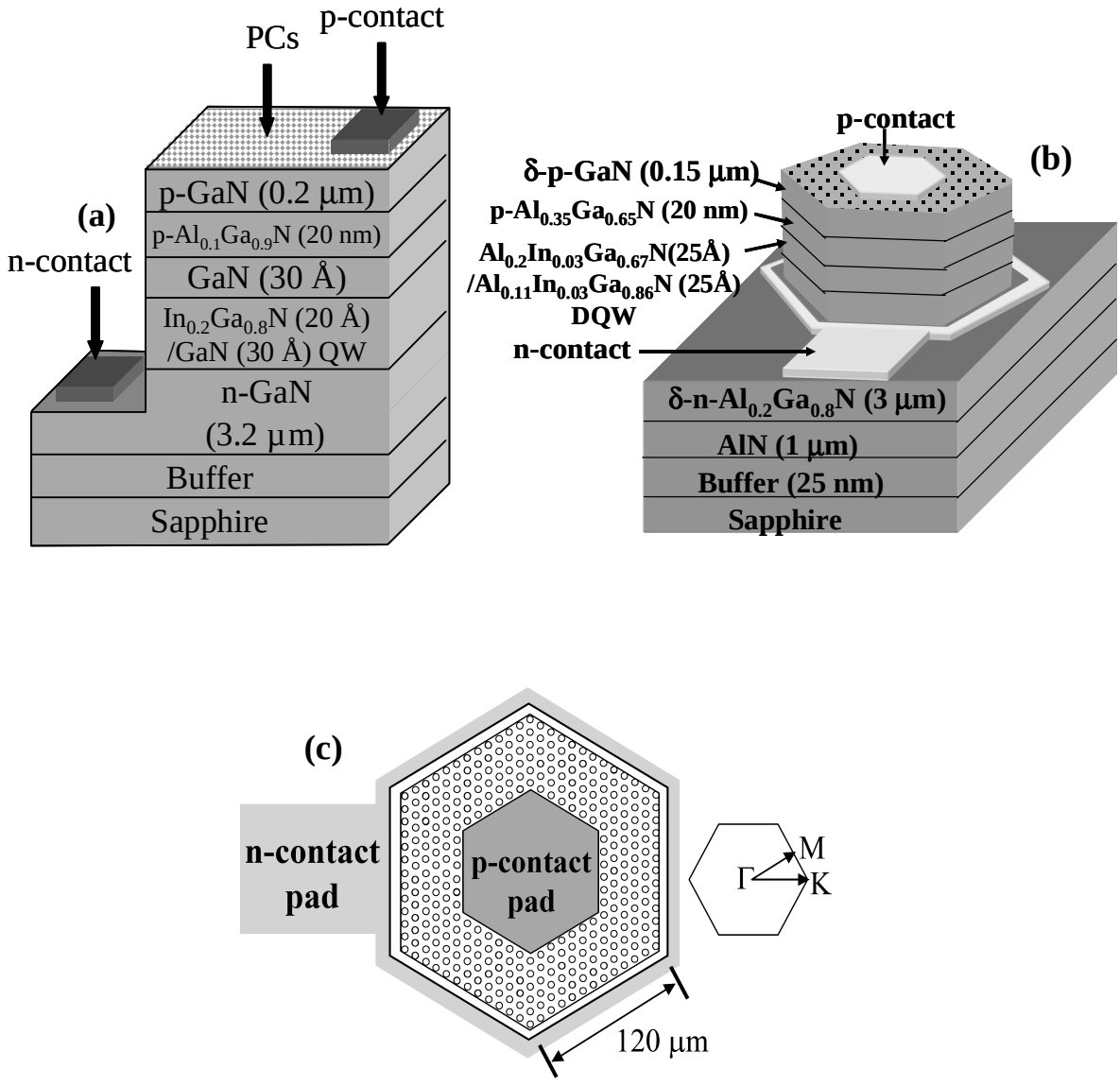

Fig. 1 Schematic diagram of (a) 460 nm blue LED structure with square mesa, and (b) 333 nm UV LED structure with hexagonal mesa. (c) Schematic top view diagram of the hexagonal mesa. The p-contact pad side length is 60 μm. Triangular array of holes were etched on top of mesa all around p-contact pad with Γ-K direction of PCs perpendicular to the side of mesa.

2.2 Characterization

The surface morphology of the etched nitride PCs was characterized using scanning electron microscopy (SEM) and atomic force microscopy (AFM). For optical measurements, laser light of wavelength 266 nm was focused to a small spot size of about 3 μm on the sample using the NSOM system specially configured for UV wavelengths. The laser light was pumped on the unpatterned area of the sample about 10 μm outside the PCs and the emission intensity collected by the NSOM tip placed above the PCs. Emission intensity was also collected at an equal distance away from the same pump spot in an unpatterned region of the sample. The experimental set-up for this measurement, illustrated in Fig. 2, would thus enable direct comparison between emission light intensity collected at the MQW region patterned with PCs and an unpatterned region. This set-up is similar to the one used by Boroditsky et al[10], where light generation region is separate from extraction region patterned with PCs since improvement is sought for light extraction as opposed to spontaneous emission. I-V, L-I and electroluminescence (EL) measurements on specific LEDs were taken before and after the fabrication of PCs for comparison.

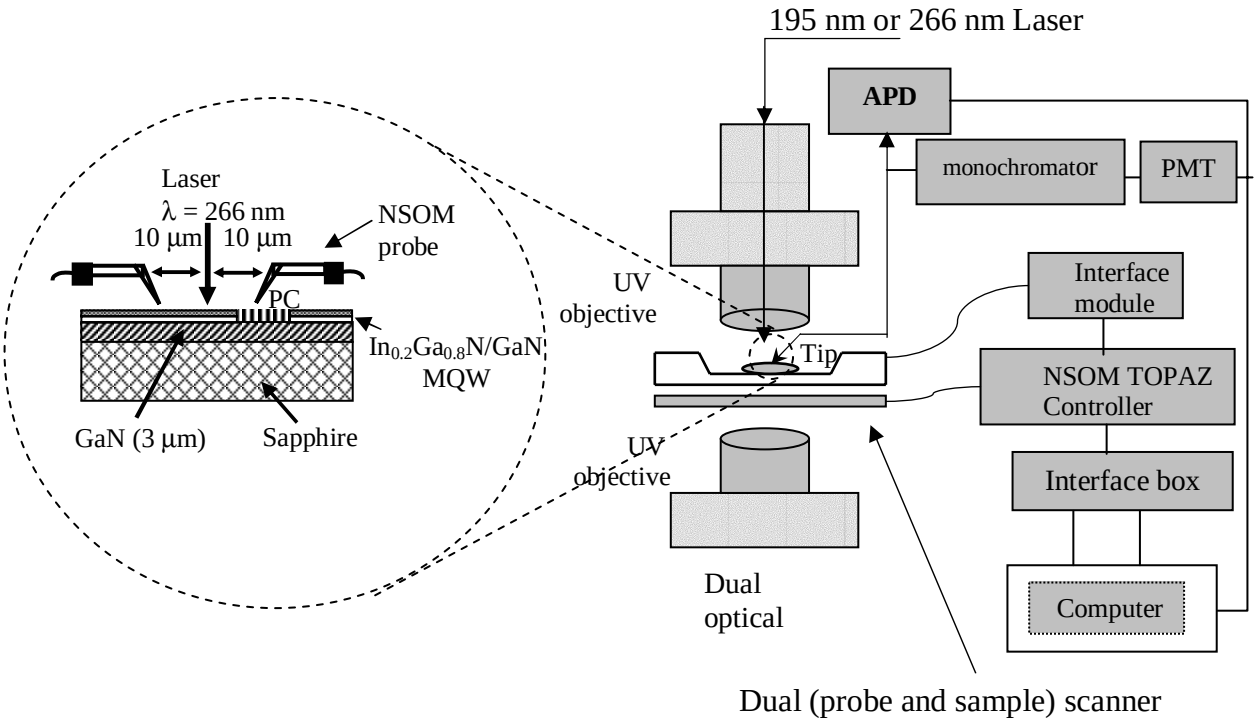

Fig. 2 : Schematic set-up of NSOM measurement of the light extraction by PCs. A magnified schematic of the sample is shown in the left.

3. RESULTS AND DISCUSSIONS

Fig. 3 (a) and (b) show the SEM images of the nitride PCs after the patterns were etched into the InGaN/GaN MQWs with a = 180 nm, d = 100 nm and a = 300 nm, d = 120 nm respectively. The later structure with a = 300 nm, d = 120 nm and an air-filling factor of 29% was optically pumped using NSOM. . Fig 3(c) shows the 60° tilted SEM image of the PCs with a = 600 nm and d = 400 nm etched on UV LED (λ = 313 nm). Atomic force microscopy (AFM) image of the PCs on UV LED (λ = 333 nm) with a = 600 nm and d =200 nm is shown in Fig 3(d). The targeted etching depth of the holes was 200 nm. AFM image revealed that the depth of the etched holes varied from 175 nm to 190 nm and that

the holes with larger diameter were etched relatively deeper. This indicates that most of the holes were etched through to the active layers

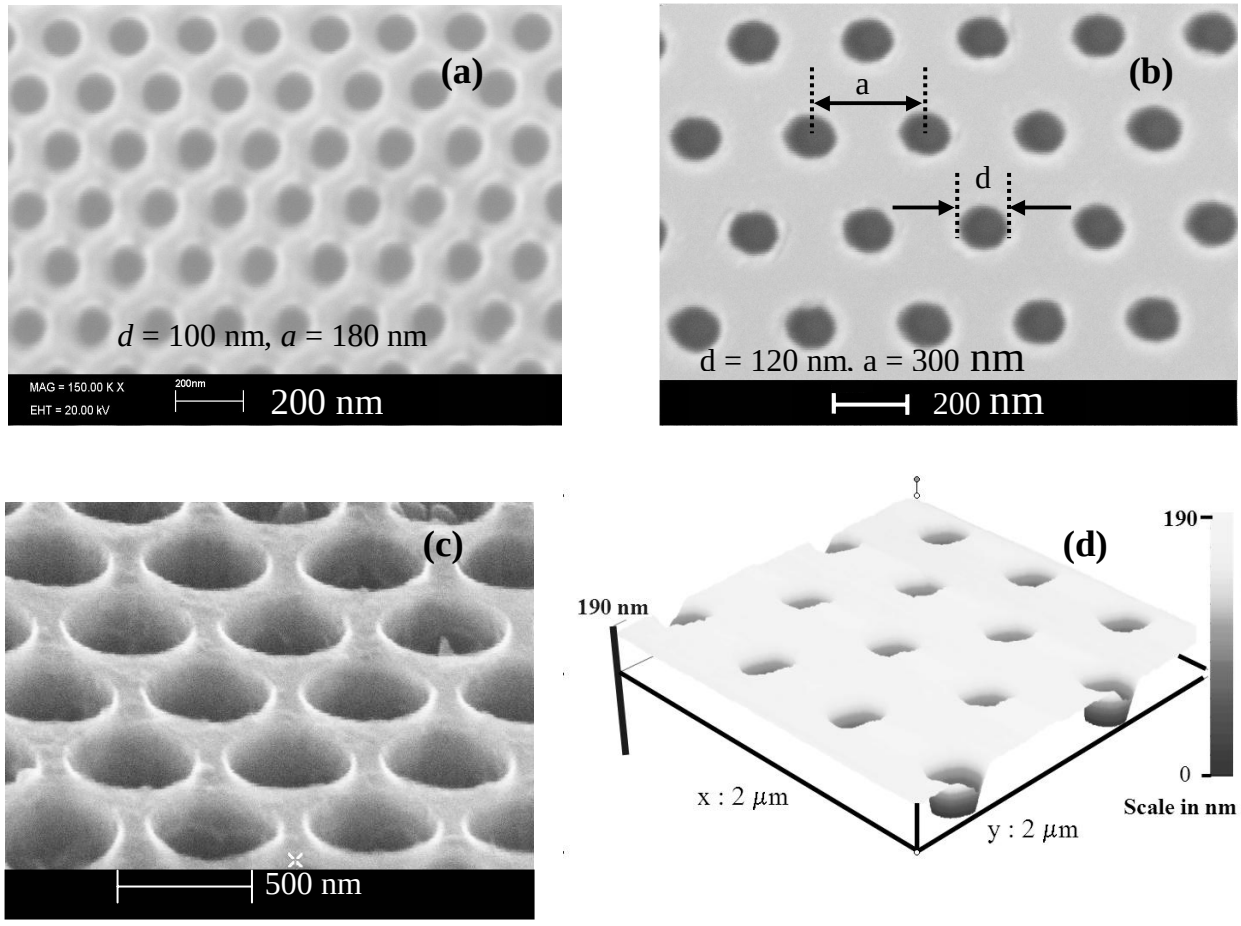

Fig. 3 SEM images of nitride PCs (a) with a = 180 nm, d = 100 nm, (b) with a = 300 nm, d = 120 nm. (c) 60^{o} tilted SEM image of PCs on 313 nm UV LEDs with a = 600 nm, d = 400 nm. (d) AFM image of PCs on 333 nm UV LEDs with a = 600 nm, d = 200 nm.

3.1 Optical pumping of PCs on InGaN/GaN MQW using NSOM

Fig. 4 shows the photoluminescence (PL) spectra at T = 300 K for the two cases depicted in the magnified schematic of Fig. 2 above, with the propagation direction of emission light from the laser pump spot parallel to the Γ-K lattice direction of the PCs. The emission peak at 475 nm is attributed to the localized exciton recombination in the well regions of the MQW structure. From this figure, the region patterned with PCs produced an enhancement of the emission intensity of about twenty times compared to the unpatterned region of the sample. The enhancement factor of 20 at room temperature is, to our knowledge, the largest value so far reported for semiconductor PCs. Fig. 5(a) shows a 3D NSOM intensity image collected above the 12 μm x 12 μm region patterned with PCs using the NSOM setup shown in Fig. 2. The blue color represents the lowest intensity, whereas the red color represents the highest intensity in the 3D NSOM image. The laser pump spot was located about 30 μm away from the PCs in the unpatterned region of the sample. The line scan across the 3D NSOM image of Fig 5(a) is plotted in Fig. 5(b) and shows increase on the NSOM intensity scale from about 7 units in the unpatterned region of the MQW to 135 units in the region of the MQW with PCs giving an enhancement factor consistent with the PL data shown in Fig. 4.

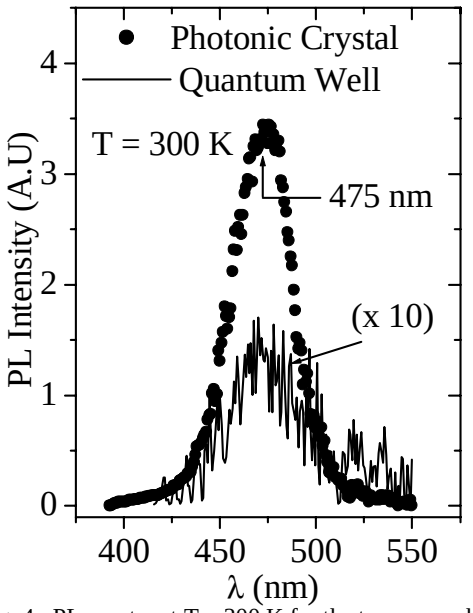

Fig. 4: PL spectra at T = 300 K for the two cases shown above in Fig. 2, measured by NSOM in collection mode.

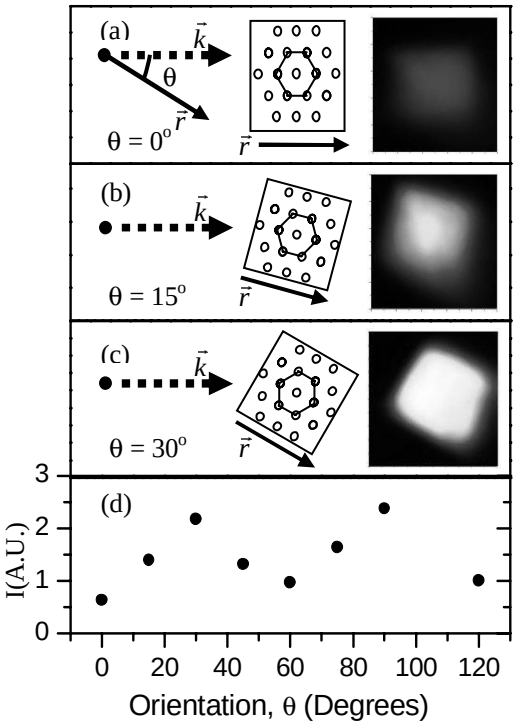

Fig. 6: Illustration of the set-up and the scanned NSOM intensity image across the PC region for three different orientations θ = 0°, 15° and 30° respectively. A plot of NSOM intensity versus θ is shown in (d) and indicates a 60° periodicity where the NSOM intensity is minimum for θ = 0° or 60° corresponding to Γ-M direction, and maximum for θ = 30° or 90° corresponding to Γ-K direction.

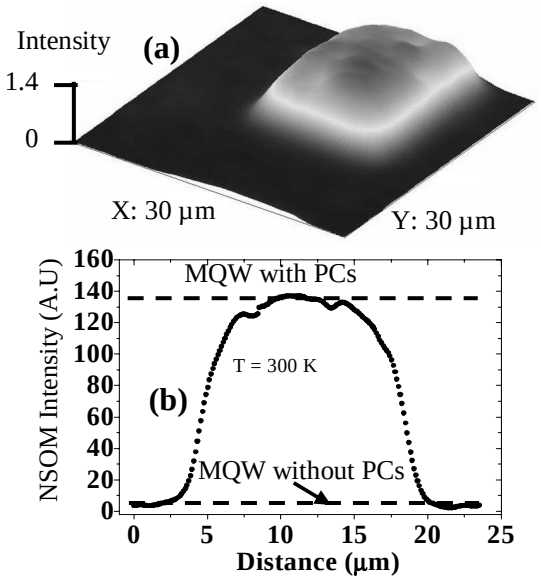

Fig. 5: (a) 3-dimensional NSOM intensity image collected above the 12 μm x 12 μm region patterned with PCs. (b) Line scan across the NSOM image showing increase in intensity from about 7 units in the unpatterned region of the MQW to about 135 units in the region of the MQW with PCs.

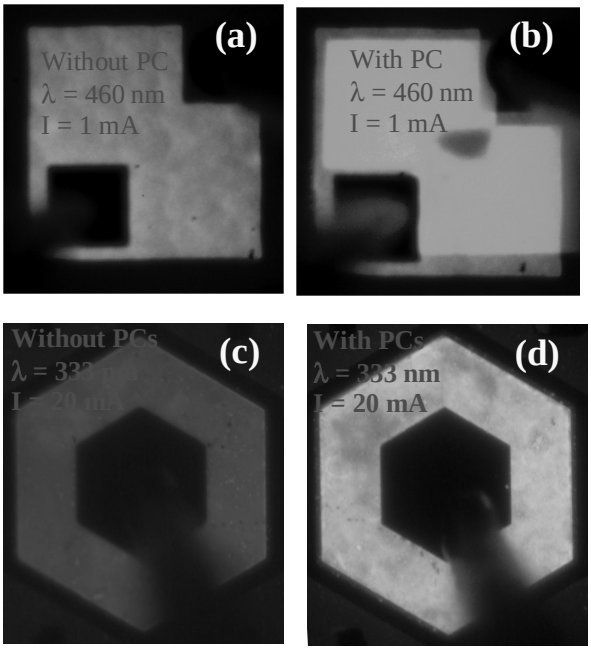

Fig. 7: Optical microscopy (CCD) images of 300 x 300 μm^2 blue LED (λ = 460 nm) (a) without and (b) with PCs (*a*=700 nm, *d*=300 nm), both under 1 mA electrical current injection. The CCD images of hexagonal mesa UV LEDs (λ = 333 nm) at 20 mA current injections (c) without PCs, (d) with PCs (*a*=600 nm, *d*=200 nm). The darker area in the right bottom side of both lower images is due to the light obstruction by the p-contact probe.

There are two possible ways by which PCs can improve LED output power. The first is by the Purcell spontaneous emission rate enhancement due to band structure and nanocavities of the PCs. Purcell enhancement factor, f, is defined as[19,7]

$$f = \frac{3Qg(\lambda/2n)^3}{2\pi V_{CAV}} \quad (1)$$

where Q is the quality factor, g is mode degeneracy, λ is the wavelength, n is the refractive index, and V_{cav} is the cavity volume. Q is limited to 10 - 30 at room temperature by the material properties of the semiconductor[7]. For the nitride materials, n ~ 2.4 and at a wavelength of 475 nm, $V_{cav} \approx 0.0024\ \mu m^3$. These lead to a maximum f value of about 5.7 for single mode degeneracy, implying that overall improvement of LED operation by Purcell effect may be limited.

The second method through which PCs can improve LED output power is by Bragg scattering, which is directly related to extraction efficiency. Light extraction in this case is enhanced in two possible ways[10]. Firstly, the creation of the 2D PBG forbids the lateral guided modes in the bandgap region thus forcing the emitted power to couple to free space modes and radiate out of plane[20,21]. The mid-gap frequency of the PBG of triangular PCs of air hole in GaN (with dielectric constant ε ~ 8) is estimated to be around the normalized frequency (a/λ) of 0.5.[22] A periodicity of less than 240 nm is required to tune the PBG to the emission wavelength λ = 475 nm of the structure. Secondly, the photonic crystal periodicity folds the higher momentum guided modes, which lie below the air light line defined by $\omega = c\,|k_o|$ with k_o being the in-plane wave vector in air, to the first Brillouin zone. The folded guided mode that lies above the air light line can phase match to radiation mode and leak out as Bragg scattered light[7, 20]. For triangular lattice of air hole, all the modes above normalized frequency $a/\lambda = 0.66$ (i.e. all $\lambda < 1.51\ a$) will be Bragg scattered. The normalized frequency corresponding to our structure (a = 300 nm, d = 120 nm) is 0.63 for a wavelength of 475 nm and most of the photon modes in our structure lie above the cut-off frequency (air light line) of the guided modes. We therefore believe that the enhancement in our measurement is mainly due to coupling to leaky modes above the cut-off frequency of the guided modes in our PCs.

The variation of the propagation direction of emission light from the MQW with the orientation of the PC lattice is shown in Fig. 6. In this measurement, the laser pump spot was about 100 μm from the PC region and the NSOM intensity was collected above the PCs in a 20 x 20 μm region enclosing the PCs. The sample was then manually turned about the vertical axis at different orientations θ (defined as an angle between laterally propagating emitted light in the MQW and Γ-M direction of the PC lattice) ranging from 0^o to 120^o. Fig. 6(a) – (c) show the illustration of the set-up and the scanned NSOM intensity image across the PC region for three different orientations, $\theta = 0^o$, 15^o and 30^o. A plot of the NSOM intensity versus orientation θ is shown in Fig. 6(d). A clear 60^o periodicity is shown in this result, where the NSOM intensity is minimum for orientation of 0^o or 60^o corresponding to Γ-M direction; and increases three-fold for orientation of 30^o or 90^o corresponding to Γ-K direction of the PCs lattice. This corresponds to an increase in enhancement factor from 7 along the Γ-M direction to 20 along the Γ-K direction. For light extraction application in LEDs, achievement of an enhancement factor of 14, being the average value over the various propagation directions we have obtained; would still be a substantial increase in extraction efficiency. A typical dispersion diagram of transverse electric (TE) modes in a triangular lattice structure of PCs reveals that the PBG along Γ-K direction is larger than that along Γ-M direction[21]. This possibly translates into a large change in enhancement factor for light traveling along the different directions as our data shows. In any case, the observed angle dependence in Fig. 6 is a direct demonstration of PBG effect of PCs.

3.2 Current injected PC-LEDs

Typical electroluminescence (EL) spectra of the 460 nm blue LEDs and 333 nm UV LEDs are shown in Fig. 8(a) and (b) respectively. No change was noticed in the peak position as well as the line-width of the EL spectrum due to PC formation indicating that the spontaneous emission is not significantly altered by the formation of PCs. Even though the holes were etched through the active layers, the PC formation was unlikely to modify the spectra as the lattice constant of the PCs is larger than the normally required value ~λ/2 (ref. 20) to tune the PBG to spontaneous emission regions.

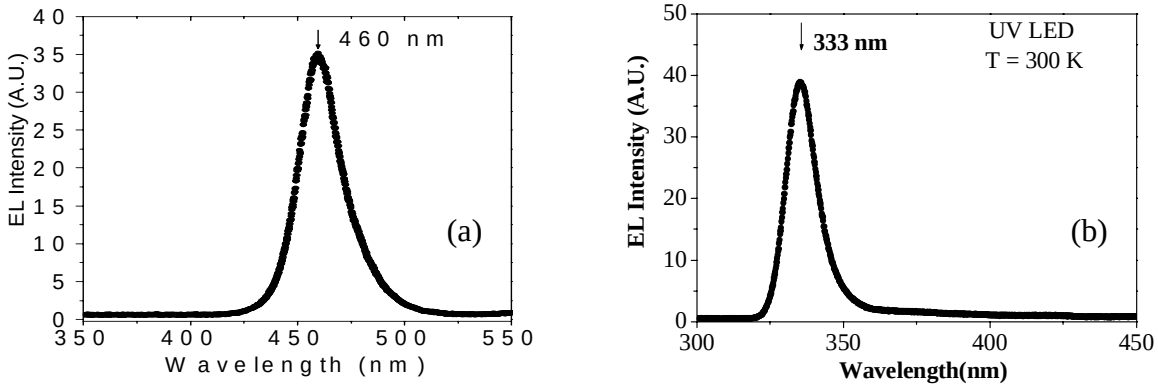

Fig. 8 Typical EL spectra from (a) 460 nm blue LEDs, and (b) 333 nm UV LEDs

3.2.1 Blue PC-LEDs

Optical microscopy images of a 300 x 300 μm^2 blue LED are shown in Fig. 7 (a)without and (b) with PCs (a = 700 nm, d = 300 nm), both under 1 mA electrical current injection. The images were taken under the same camera settings for accurate comparison. The middle part in the picture of Fig. 7 (b) with less brightness corresponds to a damaged area resulting from alignment error during e-beam writing of the PCs. The LEDs patterned with PCs become much brighter under the same current injection.

The I-V and L-I characteristics for square (300 x 300 μm^2) blue LEDs are shown in Fig. 9 (a) and (b). The forward voltage (V_F) at 20 mA current shows an increase from 4.0 V to 4.2 V for blue LEDs (Fig. 4 (a)). The slight increase in V_F for blue LEDs is attributable to reduction in total active area and p-type contact region. The optical power shown in Fig. 9 (b) was obtained by averaging the values measured from the top and bottom sides of the unpackaged LED chips. At 20 mA, the optical power of the 460 nm blue LED increased from 1.37 mW to 2.24 mW as a result of PC formation corresponding to an increase in optical power by 63% (enhancement factor =1.63).

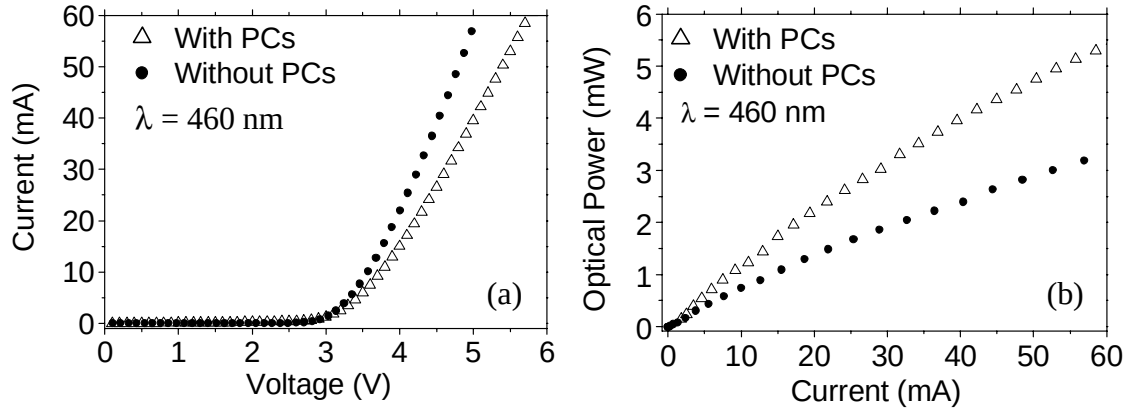

Fig. 9 (a) I-V characteristics, and (b) L-I characteristics of 460 nm unpackaged blue LEDs (300 x 300 μm^2) with PCs (a =700 nm, d=300 nm) and without PCs. The forward voltage (V_F) shows an increase by about 0.2 V and the optical power enhanced by 63% at 20 mA following patterning of PCs.

3.2.2 UV PC-LEDs

Fig. 7(c) and (d) show the optical microscopy images of UV LEDs in action at 20 mA current injections. The less bright image in Fig 7 (c) is the LED without PCs. The LED with PCs (a = 600 nm, d = 200 nm) is shown in Fig 7 (d), which clearly shows significant enhancement of light output by the LED with PCs. The current was injected by probing with needle hence the darker area in the right bottom side of both of the images is due to the light obstruction by the probe tip.

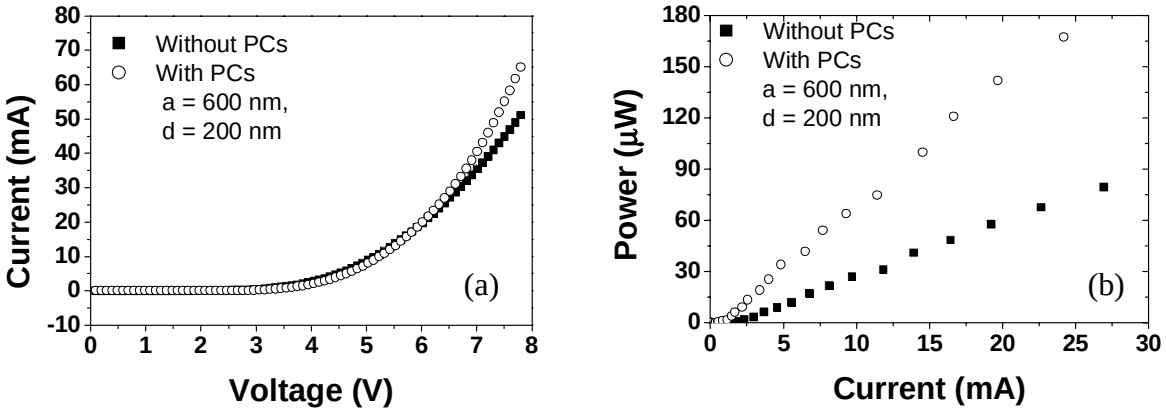

Fig. 10 (a) I-V characteristics, and without PCs and (b) L-I characteristics of 333 nm hexagonal mesa UV LEDs with PCs (*a*=600 nm, *d*=200 nm) and without PCs, measured using an integrating sphere. At 20 mA, the output power was enhanced by a factor of 2.5 in the PC-LED.

Fig 10 (a) shows the current-voltage (I-V) characteristics of 333 nm UV LEDs with PCs (*a* = 600 nm, *d* = 200 nm) and without PCs. While the operating voltages at 20 mA (V_F) for both LEDs are the same around 5.7 V, the forward current increases faster in the LED with PCs. The turn on voltage for the LED with PCs is slightly higher than that of without PCs, which can be attributed to the reduced area of the p-type material due to the formation of PC. The faster increase of the forward current for the LED with PCs may be due to the following two reasons. Firstly, the formation of PCs enhances the spontaneous emission rate in the LED due to microcavity effect or Purcell effect, which increases the carrier injection or current. The second and more probable reason for the increase in the current is the increase in the surface recombination of the injected electrons and holes as a result of increased surface around etched holes.

The output power vs injection current characteristics (L-I) of LEDs with and without PCs (*a* = 600 nm, *d* = 200 nm) is shown in Fig. 10 (b). Output power was measured using an optical integrating sphere. At I = 20 mA, the output power of UV LEDs with/without PCs are 147 μW / 60 μW respectively, giving an enhancement by a factor of about 2.5 with PCs. While the optical power level is still low for the UV LEDs studied here, comparison is being made on the overall intensity enhancement using PCs. Our most recent experiments have yielded UV LED materials that offer outputs of more than 1 mW of 300 nm radiation at 120 mA. We expect that the overall power enhancement due to PC formation will translate into those new LEDs.

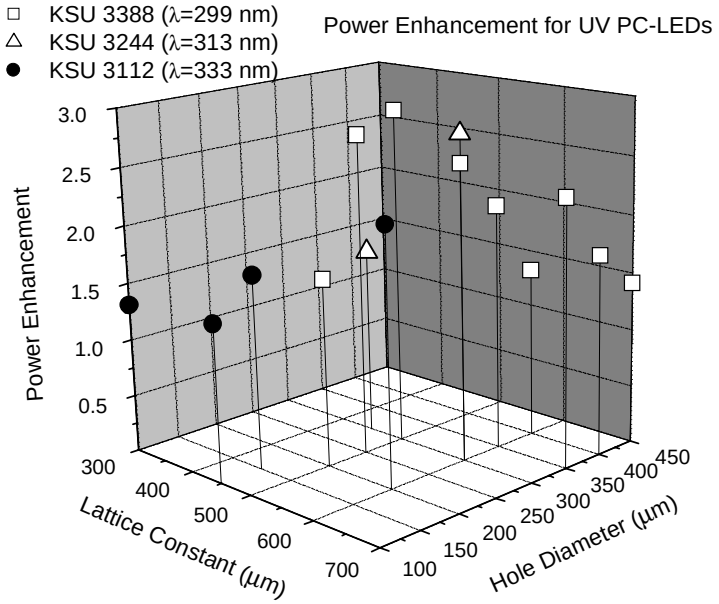

Fig. 11: 3D plot of the PCs lattice constant and the air hole diameter dependence of the enhancement factor in the UV LEDs. Three different sets of UV PC-LEDs were studied. A highest enhancement factor of about 2.9 was observed with PCs parameters *a* = 500 nm, *d* = 300 nm

Fig 11 shows the PCs lattice constant and the air hole diameter dependence of the power output enhancement factor in the UV LEDs. An enhancement factor ~2.9 was observed for 299 nm UV PC-LEDs with PCs (a = 500 nm, d = 300 nm). In contrast to expectations, we got surprisingly higher enhancement for moderately larger dimensions of lattices. This implies that the light extraction was dominated by the process of Bragg scattering instead of the effect of the PBG creation. Enhancement factor increases with d up to d = 300 nm then decreases with d. This may be due partly to the fact that the etching is not perfectly vertical and the actual hole size near the active layer is smaller than the targeted. Also, the much bigger size holes effectively remove a large portion of the active region thus reducing the power. We believe that further enhancement can be achieved by improving vertical etching.

4. CONCLUSION

We have achieved the nanofabrication of triangular lattice array of photonic crystals (PCs) with diameter/periodicity as small as 100/180 nm on III-nitride Light Emitting Diodes (LEDs). Optical pumping showed an enhancement by a factor of 20 on the emission light intensity with PCs on LEDs. Optical power enhancement factors of about 1.63, 2.5, and 2.9 were achieved for blue (λ = 460 nm, a = 700 nm, d = 300 nm), UV (λ = 333 nm, a = 600 nm, d = 200 nm), and UV (λ = 299 nm, a = 500 nm, d = 300 nm) PC-LEDs, respectively, under current injection. Our results show significant achievement in the use of PCs to realize enhanced power output in fabricated LEDs. Greater enhancement is expected with further improvement in the design and nano-fabrication processing.

5. ACKNOWLEDGEMENT

The authors wish to acknowledge support by grants from DARPA, ARO, DOE, and NSF.

6. REFERENCES

* jiang@phys.ksu.edu

[1] S. Nakamura and G. Fasol, *The Blue Laser Diode,* (Springer, Berlin, 1997):
[2] M. Boroditsky and E. Yablonovitch, *Proc. SPIE.* **3002,** 119, (1997).
[3] W. N. Carr and G. E. Pittman, *Appl. Phys. Lett.* **3,** 173, (1963).
[4] I. Schnitzer, E. Yablonovitch, C. Caneau, and T. J. Gmitter, *Appl. Phys. Lett.* **62,** 131, (1993).
[5] I. Schnitzer, E. Yablonovitch, C. Caneau, and T. J. Gmitter and A. Scherer, *Appl. Phys. Lett.* **63,** 2174, (1993).
[6] E. F. Schubert. Y.-H. Wang, A. Y. Cho, L.-W. Tu, and G. J. Zydzik, *Appl. Phys. Lett.* **60,** 992, (1992).
[7] A. A. Erchak, D. J. Ripin, S. H. Fan, P. Rakich, J. D. Joannoupoulos, E. P. Ippen, G. S. Petrich and L. A. Kolodziejski, *Appl. Phys. Lett*. **78,** 563, (2001).
[8] H. Y. Ryu, J. K. Hwang, Y. J. Lee and Y. H. Lee, *IEEE J. on Selected Topics in Quantum Electronics* **8,** 312, (2002).
[9] M. Boroditsky, T. F. Krauss, R. Coccioli, R. Vrijen, R. Bhat and E. Yablonovitch, *Appl. Phys. Lett.* **75,** 1036, (1999).
[10] M. Boroditsky, R. Vrijen, T. F. Krauss, R. Coccioli, R. Bhat and E. Yablonovitch, *J. Lightwave Technol*. **17,** 2096, (1999).
[11] T. N. Oder, J. Shakya, J. Y. Lin and H. X. Jiang, *Appl. Phys. Lett.* **83,** 1231, (2003).
[12] T. N. Oder, K. H. Kim, J. Y. Lin and H. X. Jiang, *Appl. Phys. Lett.* **84,** 466, (2004).
[13] J. J. Wierer, M. R. Krames, J. E. Epler, N. F. Gardner, and M. G. Craford, *Appl. Phys. Lett.* **84,** 3885, (2004).
[14] J. Shakya, K. H. Kim, J. Y. Lin and H. X. Jiang, "Enhanced light extraction in III-nitride ultraviolet photonic crystal light-emitting diodes" submitted to APL
[15] S. X. Jin, J. Shakya, J. Y. Lin and H. X. Jiang, *Appl. Phys. Lett.* **78,** 3532, (2001).
[16] E. Yablonovitch, *Phys. Rev. Lett.* **58,** 2059, (1987).
[17] J. Shakya, J. Y. Lin and H. X. Jiang, "Time-resolved electroluminescence studies of III-nitride ultraviolet photonic crystal light-emitting diodes", submitted to APL
[18] K. H. Kim, J. Li, S. X. Jin, J. Y. Lin and H. X Jiang, *Appl. Phys. Lett*. **83,** 566, (2003).
[19] E. M. Purcell, *Phys. Rev.* **69,** 681, (1946).
[20] S Fan, P R. Villeneuve, and J. D. Joannopoulos, *Phys. Rev. Lett.* **78,** 3294, (2000).
[21] J. D. Joannopoulos, R. D. Meade, and J. N. Winn, *Photonic Crystals, Molding the Flow of Light,* (Princeton University Press, Princeton, 1995)
[22] A. Barra, D. Cassagne and C. Jouanin, *Phys. Stat. Sol. A* **176,** 747, (1999).